Published OnlineFirst July 10, 2018; DOI: 10.1158/2326-6066.CIR-17-0698

Research Article

Cancer Immunology Research

RORγt-Expressing Tregs Drive the Growth of Colitis-Associated Colorectal Cancer by Controlling IL6 in Dendritic Cells

Angelamaria Rizzo[1], Martina Di Giovangiulio[1], Carmine Stolfi[1], Eleonora Franzè[1], Hans-Joerg Fehling[2], Rita Carsetti[3], Ezio Giorda[3], Alfredo Colantoni[1], Angela Ortenzi[1], Massimo Rugge[4], Claudia Mescoli[4], Giovanni Monteleone[1], and Massimo C. Fantini[1]

Abstract

Chronic inflammation drives colitis-associated colorectal cancer (CAC) in inflammatory bowel disease (IBD). FoxP3$^+$ regulatory T cells (Treg) coexpressing the Th17-related transcription factor RORγt accumulate in the lamina propria of IBD patients, where they are thought to represent an intermediate stage of development toward a Th17 proinflammatory phenotype. However, the role of these cells in CAC is unknown. RORγt$^+$FoxP3$^+$ cells were investigated in human samples of CAC, and their phenotypic stability and function were investigated in an azoxymethane/dextran sulfate sodium model of CAC using Treg fate-mapping reporter and Treg-specific RORγt conditional knockout mice. Tumor development and the intratumoral inflammatory milieu were characterized in these mice. The functional role of CTLA-4 expressed by Tregs and FoxO3 in dendritic cells (DC) was studied *in vitro* and *in vivo* by siRNA-silencing experiments. RORγt expression identified a phenotypically stable population of tumor-infiltrating Tregs in humans and mice. Conditional RORγt knockout mice showed reduced tumor incidence, and dysplastic cells exhibited low Ki67 expression and STAT3 activation. Tumor-infiltrating DCs produced less IL6, a cytokine that triggers STAT3-dependent proliferative signals in neoplastic cells. RORγt-deficient Tregs isolated from tumors overexpressed CTLA-4 and induced DCs to have elevated expression of the transcription factor FoxO3, thus reducing IL6 expression. Finally, *in vivo* silencing of FoxO3 obtained by siRNA microinjection in the tumors of RORγt-deficient mice restored IL6 expression and tumor growth. These data demonstrate that RORγt expressed by tumor-infiltrating Tregs sustains tumor growth by leaving IL6 expression in DCs unchecked. *Cancer Immunol Res; 6(9); 1082–92. ©2018 AACR.*

Introduction

Inflammatory bowel disease (IBD) is associated with an increased risk to develop colorectal cancer, and chronic inflammation has been shown to be the major driver of carcinogenesis (1, 2). Regulatory T cells (Treg), characterized by the expression of the transcription factor FoxP3, play a key role in the maintenance of intestinal immune system homeostasis, and loss of these cells results in an uncontrolled activation of the immune system involving different organs including the gut (3, 4). However, the role of Tregs in colitis-associated colorectal cancer (CAC) remains unclear. Data from sporadic colorectal cancer indicate that the accumulation of Tregs in the dysplastic areas is associated with both positive (5–7) and negative prognoses (8). Tregs have been reported as capable of protecting the host from cancer by reducing the inflammation mediated by T cells (9). At the same time, Tregs have shown protumorigenic effects by suppressing anticancer immune responses (10). This controversial effect may result from the presence of different Treg subsets having dissimilar functions.

In inflammatory conditions, Tregs can express specific transcription factors and cytokines that are associated with CD4$^+$ T-helper cell lineages. A specific Treg population that, together with FoxP3, expresses the transcription factor retinoic acid–related orphan receptor-γt (RORγt; ref. 11), essential for Th17 development (12), has been identified. Lines of evidence suggest that RORγt$^+$FoxP3$^+$ might represent an intermediate step of differentiation between suppressive Tregs and proinflammatory Th17 cells, and "ex-Tregs," which have lost the expression of FoxP3, have been implicated in the pathogenesis of different immune-mediated diseases (13–15). Yang and colleagues have described a microbiota-induced RORγt$^+$FoxP3$^+$ population of T cells sharing both transcriptional and epigenetic profiles of Th17 cells and Tregs. These cells represent a stable and functionally unique subset of Tregs involved in the suppression of gut-specific inflammatory responses (16). Such a population of Foxp3$^+$RORγt$^+$ cells results in their increase in the lamina propria of IBD patients compared with controls, but its functional role remains poorly defined (17). Besides the role of RORγt$^+$FoxP3$^+$ Tregs in intestinal inflammation, they are abundantly present in sporadic colon cancer in humans and mice (18). Nevertheless, the role of the Treg-specific RORγt expression in CAC is not known yet.

By using a Treg fate-mapping reporter system in the azoxymethane/destran sulfate sodium model of CAC, we demonstrated

[1]Department of System Medicine, University of Rome Tor Vergata, Rome, Italy. [2]Institute of Immunology, University Clinics Ulm, Ulm, Germany. [3]Research Centre, Bambino Gesù Children's Hospital, Rome, Italy. [4]Department of Medicine DIMED Pathology and Cytopathology Unit, University of Padova, Padova, Italy.

Note: Supplementary data for this article are available at Cancer Immunology Research Online (http://cancerimmunolres.aacrjournals.org/).

Corresponding Author: Massimo C. Fantini, University of Rome Tor Vergata, 00137 Rome, Italy. Phone: 39-06-7259-6150; E-mail: m.fantini@med.uniroma2.it

doi: 10.1158/2326-6066.CIR-17-0698

Published OnlineFirst July 10, 2018; DOI: 10.1158/2326-6066.CIR-17-0698

that FoxP3$^+$RORγt$^+$ Tregs represent a stable subset of tumor-infiltrating Tregs and that the loss of FoxP3 by these cells marginally contributed to the pool of proinflammatory RORγt$^+$ Th17 cells. RORγt expression by Tregs also contributed to tumor growth, abrogating IL6 suppression in tumor-infiltrating DCs with a mechanism involving CTLA-4 and the transcription factor FoxO3.

Materials and Methods

Mice

All the experiments involving mice were conducted in accordance with an Institutional Animal Care and Use Committee. All mice used were on C57BL/6 genetic background and were housed and bred under specific pathogen-free conditions in a facility located in Castel Romano, Rome. FoxP3eGFPCre knockin mice were kindly provided by Alexander Rudensky (MSKCC). Rosa26-tdRFP mice were provided by Hans-Joerg Fehling (University of Ulm, Germany). Rorc$^{flox/flox}$ mice were purchased from JAX. The experimental design on murine models were reviewed and approved by the local ethical committee. In order to generate the FoxP3 reporter mice, we crossed FoxP3eGFPCre knockin mice that express the green fluorescent protein (GFP)/Cre-recombinase fusion protein under control of the FoxP3 locus, with the Rosa26RFP mice carrying a reporter allele for Cre activity that expresses a nontoxic tandem-dimer red fluorescent protein (tdRFP) following Cre-mediated deletion of a floxed neo/stop cassette. RORγt FoxP3 conditional knockout mice were generated crossing FoxP3 reporter mice with rorc$^{flox/flox}$. In these mice, Cre expression, under control of the FoxP3 promoter, causes the deletion of rorc floxed exons leading to gene inactivation selectively in Tregs. The mouse strains were vital and born in the expected medelian ratios. Both the strains, the FoxP3reporter and RORγKO FoxP3reporter mice (cRORγtKO), did not show any sign of spontaneous disease up to 12 months. All animal experiments were performed in accordance with the local institutional guidelines. Male mice (6–8 weeks old) were used for all the experiments.

Human and mouse CAC immunohistochemistry and immunofluorescence

Immunohistochemistry was performed on formalin-fixed, paraffin-embedded colonic sections containing dysplastic areas from 6 patients affected by ulcerative colitis complicated by dysplasia and undergoing surgery according to current guidelines at the Department of Medicine DIMED Pathology and Cytopathology Unit, University of Padova e Registro Tumori del Veneto (Padova, Italy). Inclusion criteria for the analysis were diagnosis of ulcerative colitis and histologic evidence of dysplasia with indication to colectomy. Samples from patients affected by Crohn colitis or indeterminate colitis were excluded. The material was provided as paraffin-embedded sections and stored at room temperature until stained. The study was performed according to the principles of the Declaration of Helsinki, all participants provided written informed consent, and IRB approval (Veneto Institute of Oncology, Padova, Italy) was obtained. Human sections of CAC were deparaffinized and dehydrated through xylene and ethanol, and the antigen retrieval was performed in citrate buffer (pH 6.0) for 20 minutes in a microwave. Immunohistochemical staining was performed with the MULTIVIEW PLUS (mouse-HRP/rabbit-AP) IHC Kit Brown/Green (ENZO Life Sciences) according to the manufacturer's protocol using an anti-human FoxP3 (clone 236A/E7, eBioscience, Thermo Fisher Scientific) and an anti-human polyclonal RORC (Thermo Fisher Scientific), both final dilution 1:10 at 4°C overnight. The FoxP3- and RORC-expressing cells were counted in six high-power fields (HPF)/case using IAS 2000 System (Delta Sistemi).

Frozen sections of mouse colon containing tumoral areas were blocked in sodium tetrahydroborate (NaBH4, Sigma-Aldrich) overnight, then were blocked with goat serum for 60 minutes and incubated with rat-anti mouse IL6 (clone MP5-20F3, final dilution 1-100, Thermo Fisher Scientific), rabbit anti-mouse FoxO3 (clone K115.9, final dilution 1-100, Thermo Fisher Scientific), hamster anti-mouse CD11c (clone N418, final dilution 1-10,Thermo Fisher Scientific) in 0.1% bovine serum albumin at 4°C overnight. Subsequently, sections were rinsed with PBS and incubated with Alexa Fluor 568 (goat anti-rat–anti-rabbit) and Alexa Fluor 488 (goat anti-hamster; all 1–1,000 from Thermo Fisher Scientific) for 1 hour at room temperature in the dark. Specimens were then washed with PBS, counterstained with 4′,6-diamidino-2-phenylindole (Thermo Fisher Scientific), and sections were then mounted using Prolong Antifade kit (Thermo Fisher Scientific) and examined using a fluorescence microscope (Leica) or a confocal microscope (Nikon Instruments Spa, Eclipse TE200), with exciting at 488 nm with an Ar laser and at 542 nm with a He laser. Immunohistochemistry was performed on frozen sections of colon with tumors. Tissue sections were prepared as follows: 6-μm-thick sections were mounted onto superfrost plus glass slides (Thermo Fisher Scientific) and fixed in 4% neutral buffered formalin for 10 minutes at room temperature and then in an increasing gradient of ethanol solutions. After washing in Tris-buffered saline (Sigma-Aldrich), endogenous peroxidase activity was quenched with 3% H_2O_2 diluted in methanol for 10 minutes at room temperature. The slides were incubated with a mouse monoclonal antibody directed against mouse p-STAT3 (clone Y705, final dilution 1:100, Santa Cruz Biotechnology) or mouse Ki67 (clone MIB-5, final dilution 1 to 100, Dako, Agilent) at room temperature for 30 minutes, respectively, followed by biotin-free HRP-polymer detection (Ultravision Detection System, Thermo Scientific) with 3,3′diaminobenzidine as a chromogen (Dako, Agilent). The sections were counterstained with hematoxylin, dehydrated, and mounted. Positive cells were counted in at least 6 HPFs per section using IAS 2000 System (Delta Sistemi) and expressed as number of cells per HPF.

Azoxythane/dextran sulfate sodium (AOM/DSS) model of CAC

Mice were initially injected with the alkylating agent AOM (10 mg/kg; Sigma-Aldrich) intraperitoneally to induce mutagenesis in the gut epithelial cells. This was then followed by three cycles of 2% DSS (MP Biomedicals, 36,000–50,000) given in the drinking water for 7 days every 2 weeks to mimic relapsing colitis typically observed in human IBD. In this model, adenomas with high-grade dysplasia developed by day 30.

Endoscopic procedures

The development of tumors in mice was assessed by micro-endoscopy (Coloview). In brief, mice were weekly scoped under general anesthesia by using isofluorane vaporizer. Tumors were counted and their size quantified based on how much room of the

Published OnlineFirst July 10, 2018; DOI: 10.1158/2326-6066.CIR-17-0698

colon lumen was occupied by the tumoral mass as previously described (19).

Histologic analysis of colon cross-sections

Colonic cross-sections were obtained at the end of the experiment (day 80) and stained with hematoxylin and eosin (H&E). The severity of inflammation was semiquantitatively graded by two blinded readers as reported by Ito R and colleagues (20). Briefly, epithelial damage was scored from 0 to 4 based on the loss of goblet cells and crypts depletion. Inflammatory cell infiltration was scored from 0 (infiltration limited to the crypt base) to 4 (infiltration extended to the submucosa). Distal and proximal halves of the colon were scored separately. The final score was obtained by summing the two subscores of the two segments together.

Cell isolation

Tumor-infiltrating lymphocytes (TIL) from the tumor were obtained according to the Lamina Propria Dissociation kit mouse protocol (catalog #130-097-410; Miltenyi Biotech). Briefly, tumors were collected at the end of the experiment (day 80). Three consecutive washes were performed using Hank's balanced salt solution without Ca^{2+} and Mg^{2+} supplemented with 10 mmol/L HEPES, 5 mmol/L EDTA, 5% fetal bovine serum (FBS), and 1 mmol/L DTT in 1640 RPMI at 37°C for 20 minutes under continuous rotation on a MACSmix tube rotator to detach epithelial cells. The remaining tumor fragments were loaded into Miltenyi's C tubes containing a house made digestion buffer. C tubes were immediately processed on the Miltenyi's gentleMACS Dissociator using the tumor dissociation protocol. The cells suspension was then used for further analysis. DCs were isolated from the spleens of 8- to 10-week-old wild-type (WT) C57BL/6 by mechanical dissociation using two sterile glass slides. CD11c were magnetically sorted from the obtained splenocytes suspension using the CD11c MicroBeads UltraPure (catalog #130-108-338; Miltenyi Biotech). More than 95% pure CD11c cell population was obtained after two passages through the columns. Tumoral Tregs were sorted by a FACSAriaII (BD Biosciences) based on FoxP3eGFP and tdRFP fluorescence, obtaining a 97% to 99% pure Treg population.

Cell culture

A total of 10^5 splenic WT $CD11c^+$-enriched DCs were cultured in a 96-well plate U bottom (Falcon, calatog #353077) in RPMI 1640 supplemented with 10% FBS, 1% penicillin/streptomycin (all from Lonza). Cells were activated by the addition of LPS (100 ng/mL; Sigma) for 6 hours, and then were cocultured with 10^5 Tregs sorted from colonic tumors of WT and cRORγtKO mice for 6 hours. In some experiments, neutralizing anti–CTLA-4 (1 μg/mL; R&D Systems) was added to the culture medium described above for the entire duration of the experiment. To silence FoxO3 in DCs, 10^5 splenic $CD11c^+$-enriched cells were transfected with FoxO3-specific siRNA (mouse FoxO3 siRNA ID: s80660, Ambion, Thermo Fisher Scientific) or control oligonucleotide (scramble siRNA ID:AM4611 Ambion, Thermo Fisher Scientific) for 24 hours and then cocultured with Tregs sorted from the tumors of WT and cRORγtKO for 6 hours.

Flow cytometry

TILs (10^6) were stained with surface fluorochrome-conjugated antibodies against: CD3 (clone 500A2) and CD4 (clone GK1.5; both from BD Pharmingen), and CD80 (clone 16-10A1) and CD86 (clone GL-1; both from Tonbo Biosciences). Lineage staining was performed using antibodies against: CD11b (clone MI/70), CD11c (clone HL3), and CD19 (clone 1D2; all BD Pharmingen). Permeabilization and intracellular staining with conjugated anti-RORγt (clone Q313778) and anti-IL6 (clone MP5-20F3; both from BD Pharmingen) and CTLA-4 (clone UC10-4F10-11; Tonbo Biosciences) were performed after 5 hours of stimulation with phorbol 12-myristate 13-acetate (PMA; 40 ng/mL) and ionomycin (1 μg/mL; Sigma-Aldrich) in the presence of monensin (2 nmol/L; eBioscience, Thermo Fisher Scientific) according to the Transcription buffer Ruo set protocol (BD Pharmingen; catalog# 562574). Cells were analyzed by flow cytometry (FACS VERSE; BD Biosciences), gating on living cells according to LIVE/DEAD staining (catalog #34957; Thermo Fisher Scientific). Flow cytometry data were analyzed by FlowJo ver 10.4 (FlowJo).

In vivo FoxO3 silencing

FoxO3 siRNA (mouse siRNA ID: s80660, Ambion, Thermo Fisher Scientific) or control oligonucleotide (scramble siRNA ID: AM4611 Ambion, Thermo Fisher Scientific) were incubated in a final volume of 50 μL of saline containing 25 μL of siRNA (10 μmol/L) plus 25 μL of Lipofectamin 3000 (Transfection Kit, Invitrogen, Thermo Fisher Scientific) for 10 minutes at room temperature before injection. At the end of the AOM/DSS protocol (day 80), colonic tumors were identified, and a pretreatment biopsy was collected by endoscopy. The day after, mice underwent the intratumoral injection at the same site of biopsy with 10,000 or 1,000 nmol/L FoxO3 or control siRNA as indicated. A total volume of 50 μL was injected in each tumor with a 32-gauge needle. Endoscopy and biopsy collection was performed at 24 and 48 hours after injection and included in NEG-50TM (Thermo Fisher Scientific) for immunohistochemical analysis or stored in RNAlater (Ambion, Thermo Fisher Scientific) for total RNA extraction.

RNA extraction, complementary DNA preparation, and real-time PCR

Total RNA was isolated with the PureLink RNA Micro Kit (Thermo Fisher Scientific) for *in vitro* experiments and with PureLinkRNA Mini Kit (Thermo Fisher Scientific) for tissue according to the manufacturer's recommendations. RNA concentration was measured by using NanoDrop (Thermo Fisher Scientific). Total RNA (500–1,000 ng) was reversed transcribed into cDNA by Superscript III Reverse Transcriptase kit (Thermo Fisher Scientific), according to the manufacturer's protocol and then amplified by real-time PCR using iQ SYBR Green Supermix (Bio-Rad). PCR was performed by using the primer sets listed in Supplementary Table S1. All primers sequences were designed in-house and purchased from Applied Biosystems (Thermo Fischer Scientific). IL21 RNA expression was evaluated using a TaqMan assay (Applied Biosystems, Thermo Fisher Scientific). qPCR was performed using CFX96 Real-Time System (Bio-Rad) and RNA expression was calculated relative to the housekeeping beta-actin gene expression on the base of the ΔΔCt algorithm. Duplicates of each sample were run in all qPCRs.

Statistical analysis

Results were analyzed by two-tailed Student *t* test for parametric variables and Mann–Whitney test for nonparametric variables using GraphPad Prism 6. No statistical corrections were applied.

Published OnlineFirst July 10, 2018; DOI: 10.1158/2326-6066.CIR-17-0698

Statistical significance was indicated when $P < 0.05$, unless otherwise indicated.

Results

TILs are enriched for FoxP3$^+$RORγt$^+$ Tregs in human and murine CAC

FoxP3$^+$RORγt$^+$ cells are present in the lamina propria of IBD patients (17). To assess whether this subset of T cells accumulated in CAC, colonic sections of human ulcerative colitis containing dysplastic areas were stained for FoxP3 and RORγt. As expected, double-positive cells were observed in the lamina propria of nondysplastic areas, but a significantly higher number of these cells were quantified within the dysplastic areas of the same patient (Fig. 1A). To assess whether FoxP3$^+$RORγt$^+$ cells represented precursors of protumorigenic Th17 cells in the CAC microenvironment, we used a fate-mapping FoxP3 reporter mouse. In these mice, FoxP3$^+$ Tregs are characterized by the coexpression of both GFP and RFP, whereas Tregs that have lost FoxP3 expression do not express GFP but retain RFP. Therefore, this model makes it possible to discriminate Tregs from exTregs *ex vivo* on the basis of their endogenous fluorescence. FoxP3 reporter mice were treated with AOM/DSS as described in Fig. 1B. As expected, at the end of the experiment (day 80), mice developed multiple tumors with high-grade dysplasia (Fig. 1C and D). By gating on CD4$^+$RORγt$^+$ tumor-infiltrating cells (Fig. 1E), we observed that about one third of these cells were represented by FoxP3$^+$RORγt$^+$ Tregs (31.3%; range, 19.5%–35.6%), whereas only a small fraction of FoxP3eGFP-tdRFP$^+$ ex-Tregs (3.73%; range, 2.28%–9.45%) contributed to the pool of CD4$^+$RORγt$^+$ T cells (Fig. 1F). Given the small number of ex-Tregs expressing RORγt, these results indicate that the FoxP3$^+$RORγt$^+$ Tregs that infiltrated the tumors represent a stable population of cells rather

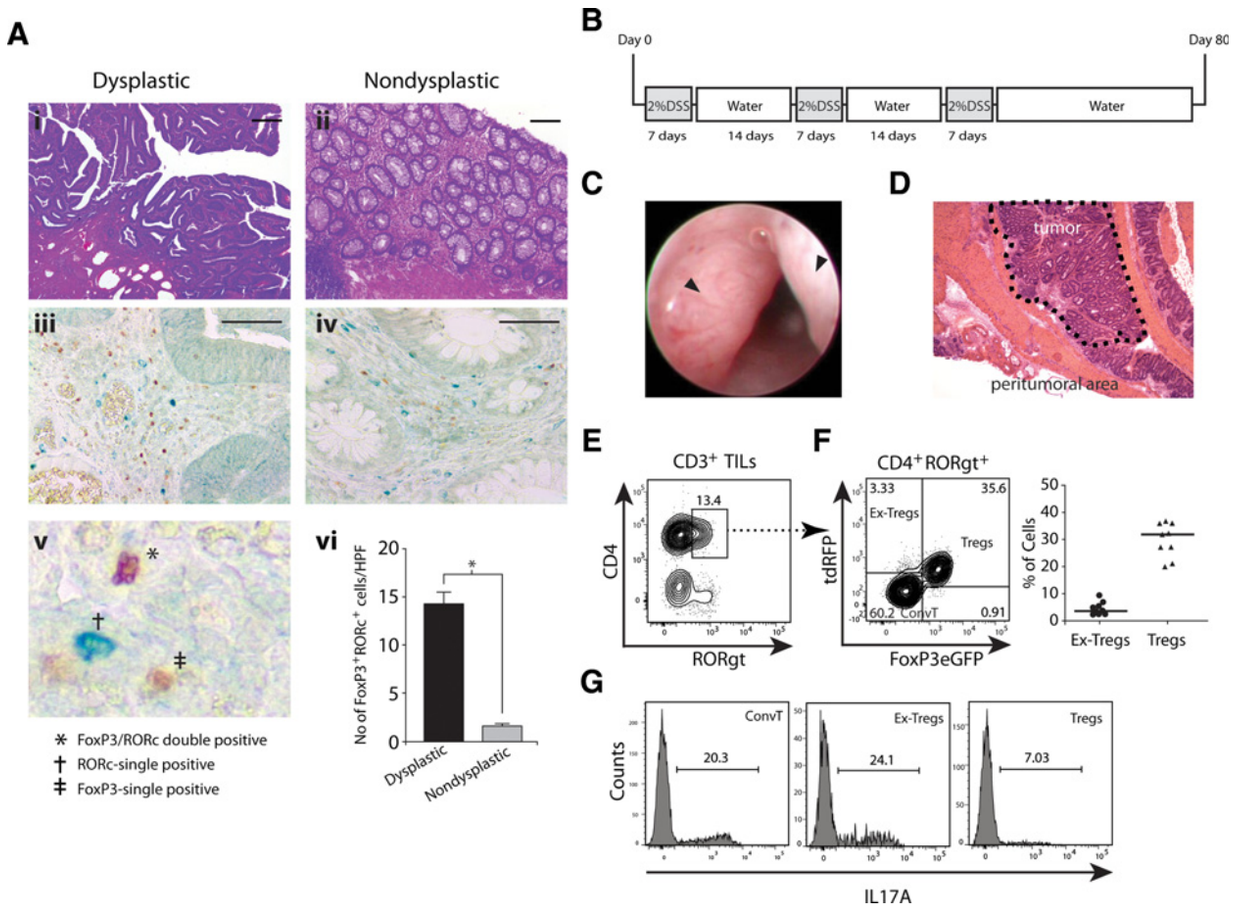

Figure 1.

Colitis-associated dysplastic areas contain a stable subpopulation of Tregs coexpressing the transcription factors FoxP3 and RORγt in humans and mice. **A,** Representative H&E stains of sections from ulcerative colitis patients complicated by dysplasia showing (i) dysplastic and (ii) nondysplastic areas. (v) Trichronic stainings showing FoxP3 single-positive (brown), RORc single-positive (blue), and FoxP3$^+$RORc$^+$ cells (violet) from (iii) the dysplastic and (iv) nondysplastic areas. (vi) Quantification of double-positive cells from 3 HPF from 6 patients. Two-tailed Student *t* test was used; *, $P < 0.05$. Scale bars, 100 μm. **B,** Schematic overview of the protocol used to induce CAC in mice. **C,** Representative endoscopic pictures (arrow heads indicate tumors) and (**D**) H&E-stained sections of dysplastic tumors from WT mice at day 80. **E,** Representative plot gated on live CD3$^+$ Lineage (Lin)$^-$ T cells isolated from tumors at day 80. Quadrant: CD4$^+$RORγt$^+$ T cells. **F,** Left, Representative plot of gated cells from **E**. Right, Cumulative results from three independent experiments ($n = 9$) showing the frequency of Tregs (FoxP3eGFP$^+$tdRFP$^+$) and ex-Tregs (FoxP3eGFP$^-$tdRFP$^+$). **G,** Representative histogram of IL17A expression in CD3$^+$CD4$^+$ ConvT, ex-Tregs, and Tregs. Numbers in the quadrants represent the frequency of gated cells. Horizontal bars, median frequency of cell subsets.

Published OnlineFirst July 10, 2018; DOI: 10.1158/2326-6066.CIR-17-0698

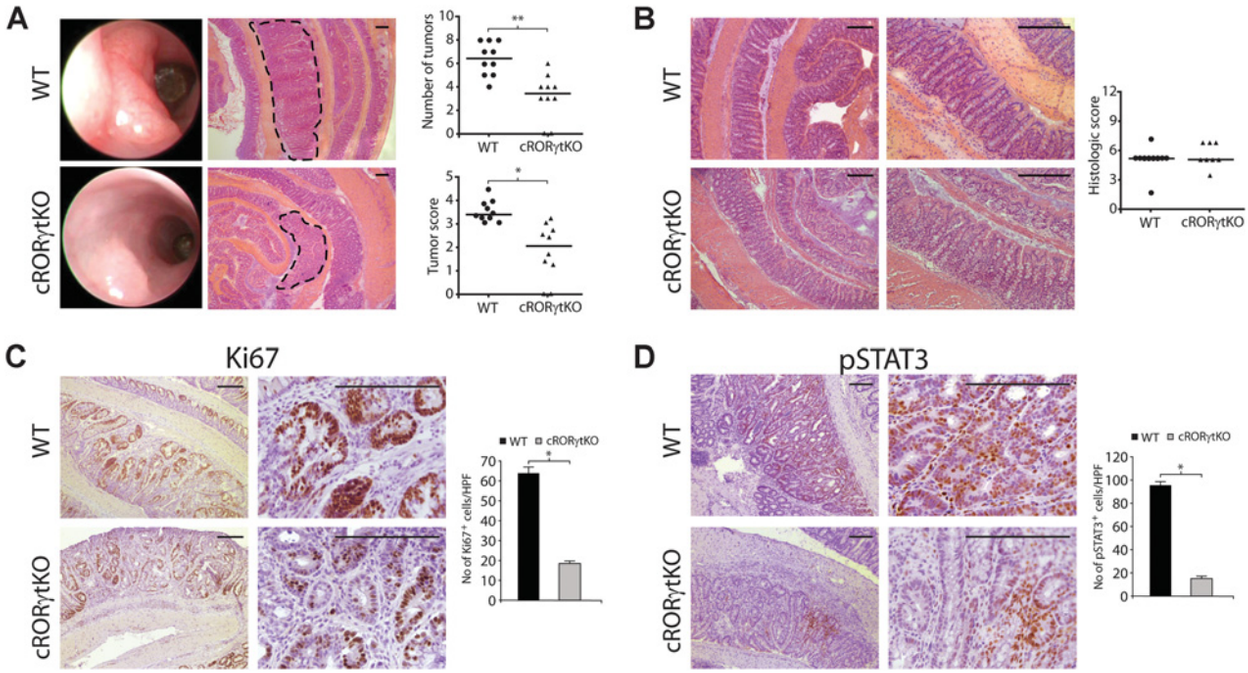

Figure 2.

cRORgtKO mice are resistant to tumor development, and dysplastic cells show low pSTAT3 and Ki67 expression. **A,** Representative endoscopic pictures (left) and H&E staining of colonic tumor sections (central) from WT and cRORγtKO mice at day 80. Dotted line, Dysplastic areas. Right, Number of tumors/colon and tumor score of WT ($n = 10$) and cRORγtKO ($n = 8$) mice. **B,** Representative H&E stainings of peritumoral areas (50× magnification left and 100× magnification center) from WT mice and cRORγtKO mice. Right, Histologic score of colitis severity analyzed in WT ($n = 10$) and cRORγtKO ($n = 8$) mice. Horizontal bars, Median value from three independent experiments. Representative (**C**) Ki67 and (**D**) pSTAT3 immunohistochemical stainings of colonic sections containing dysplastic areas from WT and cRORγtKO mice (100× magnification left; 400× magnification center). Right, Quantification of positive cells. Scale bars, 200 μm. Bars, means ± SEM. 6 HPF/section were analyzed from 6 mice/group. Two-tailed Student *t* test was used in **A,** and two-tailed Mann–Whitney was used in **F**. *, $P < 0.05$; **, $P < 0.01$.

than a step of transition toward a Th17 phenotype. We next investigated whether RORγt expression in Tregs induced IL17A, the hallmark cytokine of Th17 cells. As shown by flow cytometry, about 7% of RORγt-expressing Tregs produced IL17A. In contrast, RORγt$^+$ ex-Tregs expressed IL17A comparable to that of conventional T (ConvT) cells (Fig. 1G).

RORγt depletion in Tregs reduces tumor incidence and growth

In order to investigate the *in vivo* functional role of RORγt in Tregs, Treg-specific RORγt conditional knockout reporter mice (cRORγtKO mice) were generated by deleting RORγt specifically in FoxP3-expressing Tregs (Supplementary Fig. S1A and S1B). Endoscopy and histology showed that the number of tumors, as well as tumor scores, was significantly reduced in cRORγtKO mice treated with AOM/DSS in comparison with WT mice (Fig. 2A). However, histology and proinflammatory cytokine expression indicated that inflammation of the peritumoral areas did not differ between WT and cRORγtKO (Fig. 2B; Supplementary Fig. S2), thus indicating that the lower tumor incidence was not due to lower inflammation in cRORγtKO mice.

We next examined whether RORγt depletion in Tregs would affect proliferation of dysplastic cells. Proliferation, based on Ki67 expression, was significantly lower in the cRORγtKO mice compared with WT mice (Fig. 2C), and the activation of the signal transducer and activator of transcription 3 (STAT3), which has been shown to be pivotal in tumor progression by increasing tumor cell proliferation in CAC (21–23), was reduced in the tumors of cRORγtKO mice compared with the WT control group (Fig. 2D). Overall, these findings indicate that the expression RORγt in Tregs sustained tumor development, dysplastic epithelial cell proliferation, and STAT3 activation.

IL6 expression is downregulated in the tumors of cRORγtKO mice and restricted to activated DCs

To unravel which factor was responsible for STAT3 activation in the epithelial cells, the expression of a panel of cytokines (i.e., *Il6*, *Il11*, *Il17a*, *Il21*, *Il22*, and *Tnf*) known to activate STAT3 and involved in tumor cell growth was analyzed (21, 22, 24–27). Among these cytokines, *Il6* was significantly reduced in the tumors of cRORγtKO mice compared with the WT (Fig. 3A). Consistent with these findings, fewer IL6-positive cells infiltrated the tumoral stroma of cRORγtKO mice as compared with WT mice (Fig. 3B). Although neither the frequency of CD11c$^+$ DCs (Fig. 3C) nor the expression of the activation marker CD86 by these cells differed between the two groups of mice (Fig. 3D, top left), the expression of IL6 by activated CD11c$^+$CD86$^+$, but not CD86$^-$, DCs in the dysplastic area of cRORγtKO mice was significantly reduced compared with controls (Fig. 3D, bottom left and right). Accordingly, IL6-expressing CD11c$^+$ cells were reduced in the tumor sections of cRORγtKO mice compared with the WT (Fig. 3E). Expression of IL6 in tumor-infiltrating CD3$^+$ T cells did not differ in the two groups of mice (Supplementary Fig.

Published OnlineFirst July 10, 2018; DOI: 10.1158/2326-6066.CIR-17-0698

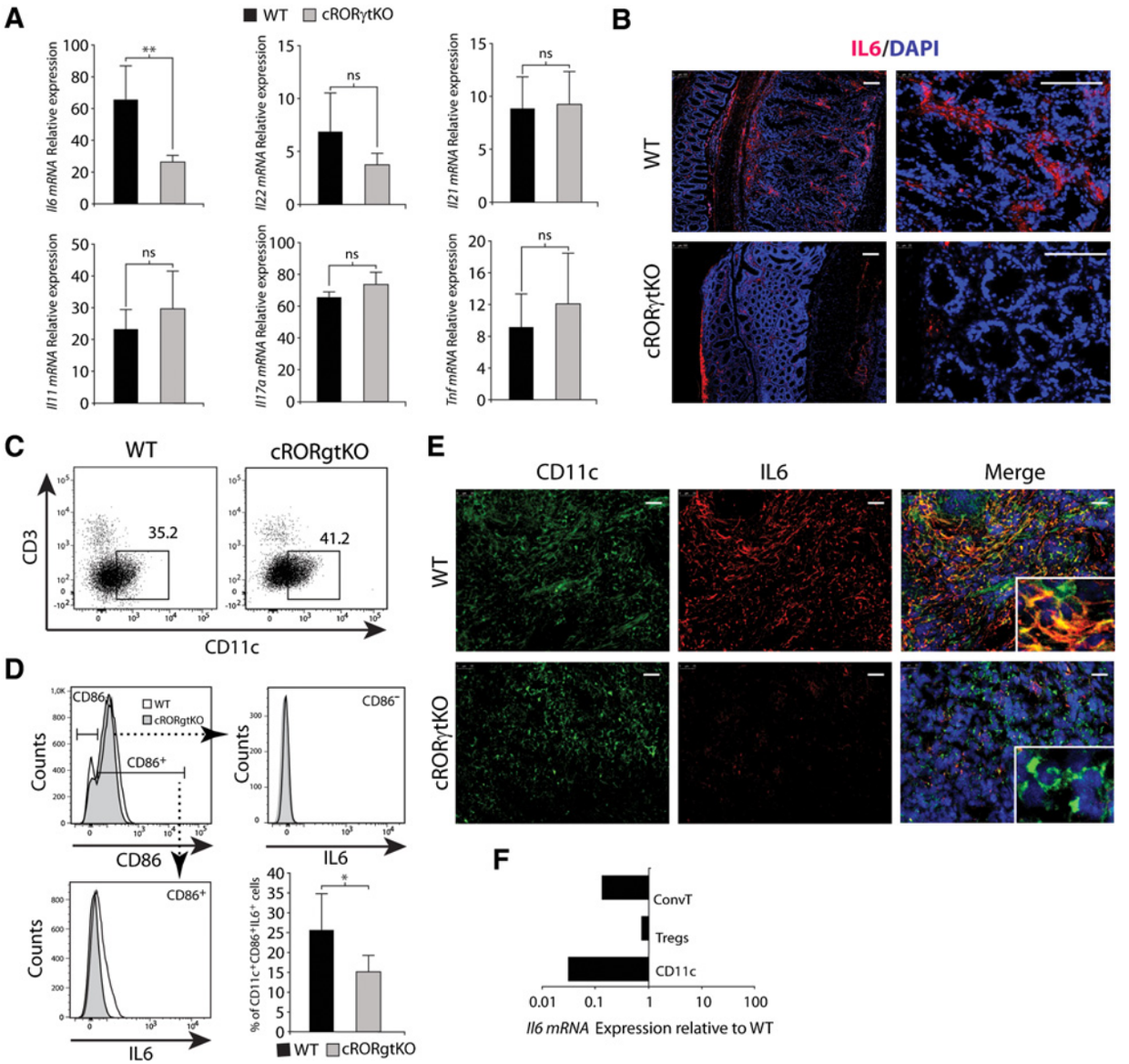

Figure 3.

Tumors of cRORγt mice are infiltrated by DCs that express low IL6. **A,** Quantification of *Il6, Il22, Il11, Il17a, Il21*, and *Tnf* mRNA expression in the tumors of WT and cRORγtKO mice. Bars, mean ± SEM. Three independent experiments using 4 to 5 mice per group. Two-tailed Student *t* test was used; **, $P < 0.001$, ns: not significant. **B,** Representative immunofluorescence of IL6 in colonic sections from dysplastic areas of WT and cRORγtKO (blue: DAPI; red: IL6). **C,** Representative plots of live CD3$^+$ and CD11c$^+$ from WT and cRORγtKO tumors. Numbers, Frequency of CD11c$^+$CD3$^-$ DCs. **D,** Top left, Representative histogram overlay gated on the live CD11c$^+$ from (**C**) showing CD86 expression in WT (black line) and cRORγtKO (filled gray). Top right and bottom left, Representative histogram overlays gated on live CD11c$^+$CD86$^+$ and live CD11c$^+$CD86$^-$ DCs showing IL6 expression in WT (black line) and cRORγtKO (filled gray). Bottom right, Frequency of CD11c$^+$CD86$^+$IL6$^+$ tumor-infiltrating cells of WT and cRORγtKO mice. Bars, mean ± SD from 3 independent experiments in which 4 to 5 mice/group were used. Two-tailed Mann–Whitney test was used; *, $P < 0.05$. **E,** Representative immunofluorescence for CD11c (green), IL6 (red), and DAPI (blue) of colonic sections containing dysplastic areas from WT and cRORγtKO mice. Scale bars, 100 μm. **F,** Representative *Il6* mRNA expression in CD3$^+$CD4$^+$ conventional T cells (ConvT), Tregs, and CD11c$^+$ cells sorted from pooled tumors of cRORγtKO mice relative to WT from one experiment of three preformed using 4 to 5 mice per group.

S3A and S3B). However, more than a 30-fold reduction of *Il6* mRNA expression was observed in DCs sorted from tumors of cRORγtKO mice compared with the WT, and *Il6* was less, but not differentially expressed, in sorted Tregs and ConvT cells (Fig. 3F), thus indicating that the modulation of IL6 by RORγt$^+$ Tregs predominantly involved DCs.

RORγt-deficient Tregs directly reduce DC-derived IL6 production

Tregs can target and suppress DC function (28). To assess whether the expression of RORγt in Tregs could directly regulate DC-derived IL6 expression, we cocultured splenic LPS-stimulated CD11c$^+$ DCs and Tregs isolated from the tumors of WT or

Published OnlineFirst July 10, 2018; DOI: 10.1158/2326-6066.CIR-17-0698

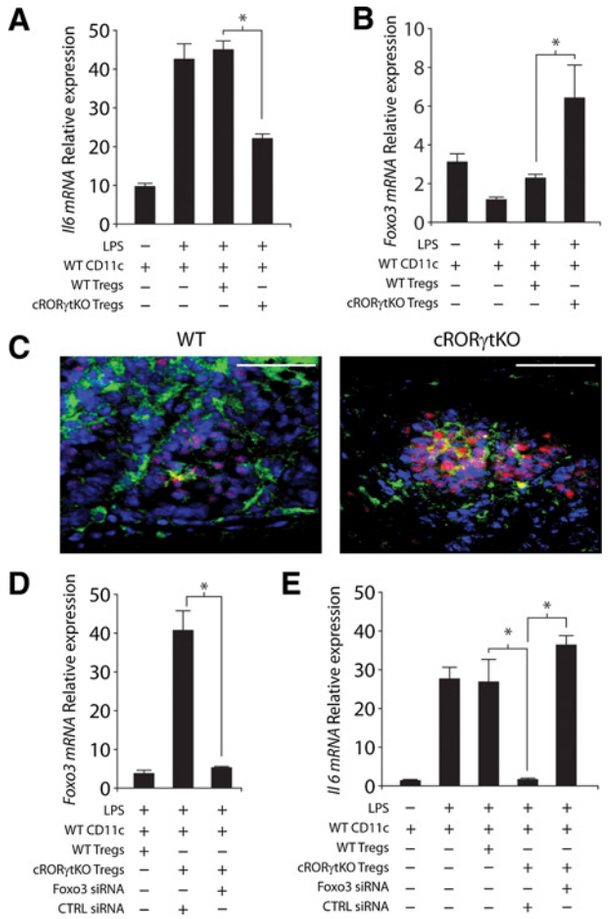

Figure 4.

RORγt depletion in Tregs directly reduces IL6 produced by DCs via a FoxO3-dependent signaling. 10^5 Splenic CD11c$^+$-enriched DCs were activated with LPS (100 ng/mL) for 6 hours and then cocultured for further 6 hours with 10^5 Tregs sorted from pooled tumors of WT or cRORγtKO mice. Representative results from three independent experiments containing 5 mice per group all used for Tregs sorting. (**A**) *Il6* and (**B**) *Foxo3* mRNA expression was analyzed by RT-PCR in cultured cells. **C,** Immunofluorescence of FoxO3 on tumor sections from WT and cRORγtKO mice (blue DAPI; green CD11c; red FoxO3). Scale bar, 100 μm. RT-PCR analysis of (**D**) *Foxo3* and (**E**) *Il6* mRNA expression in splenic CD11c$^+$ DCs transfected with FoxO3-specific or control siRNA, as indicated, and cocultured with tumor-infiltrating WT or RORγt-deficient Tregs for 3 hours. Bars, mean of duplicates ± SD of one representative experiment of three performed. Two-tailed Student *t* test was used; *, $P < 0.05$.

cRORγtKO mice. In this experiment, cRORγtKO, but not WT, Tregs significantly reduced DC-derived *Il6* (Fig. 4A). Dejean and colleagues have shown that the transcription factor FoxO3 controls IL6 production by APCs (29). Therefore, we investigated the involvement of FoxO3 in the cRORγtKO Treg-induced suppression of DC-derived IL6 synthesis. Initially, we showed that *Foxo3* expression was increased in DCs cultured with cRORγtKO but not WT Tregs (Fig. 4B). Accordingly, confocal microscopy of tumor sections showed that a greater number of CD11c$^+$FoxO3$^+$ cells accumulated in the dysplastic areas of the cRORγtKO mice compared with the WT mice (Fig. 4C). Next, we silenced FoxO3 by specific siRNA and then performed the coculture experiments as above. Inhibition of FoxO3 abrogated the inhibitory effect of cRORγtKO Tregs on DCs, restoring IL6 production at the mRNA (Fig. 4D and E) and protein levels (Supplementary Fig. S4).

RORγt deficiency in tumor-infiltrating Tregs controls CTLA-4 expression and the FoxO3-dependent suppression of IL6

Previous studies have shown that CTLA-4 signaling through the CD80/86 regulates the expression of FoxO3 in DCs (29). Therefore, we assessed whether upregulation of FoxO3 in cRORγtKO Tregs was mediated by CTLA-4 signaling. To address this issue, we initially evaluated the expression of CTLA-4 on tumoral Tregs by flow cytometry. Tregs from the tumors of cRORγtKO mice showed significantly higher mean fluorescence intensity of CTLA-4 compared with WT Tregs (Fig. 5A and B). Next, IL6 expression was evaluated in our coculture system in which CTLA-4 was neutralized by a specific recombinant mouse anti–CTLA-4 IgG. CTLA-4 blockade reduced FoxO3 expression (Fig. 5C) and upregulated IL6, even in the presence of cRORγtKO Tregs (Fig. 5D).

In vivo silencing of FoxO3 restores IL6 expression, STAT3 activation, and proliferation of tumor cells from cRORγtKO mice

To assess the *in vivo* relevance of FoxO3 in the control of IL6 expression and tumor growth, we endoscopically injected colonic

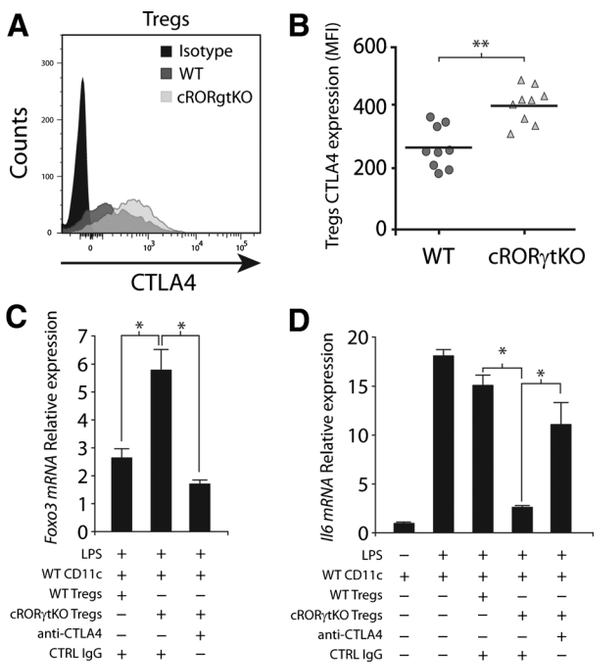

Figure 5.

CTLA-4 overexpression in cRORγtKO Treg controls FoxO3 in DCs. Representative histogram overlay gated on live CD3$^+$CD4$^+$lin$^-$eGFP$^+$tdRFP$^+$ cells showing (**A**) expression and (**B**) median fluorescence intensity (MFI) of CTLA-4 in tumor-infiltrating WT (light gray) and cRORγtKO (dark gray) Tregs. Isotype control (black). Bars, Mean ± SD from two independent experiments containing 4 to 5 mice/group. **C,** *Il6* and (**D**) *Foxo3* mRNA expression in cocultures of splenic CD11c$^+$ DCs and Tregs sorted from tumors of WT or cRORγtKO mice in the presence of anti–CTLA-4 (1 μg/mL) or isotype control as indicated. Representative results from three independent experiments containing 5 mice per group all used for Tregs sorting. Bars, mean of duplicates ±SD of one representative experiment of three performed. Two-tailed Student *t* test was used; *, $P < 0.05$; **, $P < 0.01$.

Published OnlineFirst July 10, 2018; DOI: 10.1158/2326-6066.CIR-17-0698

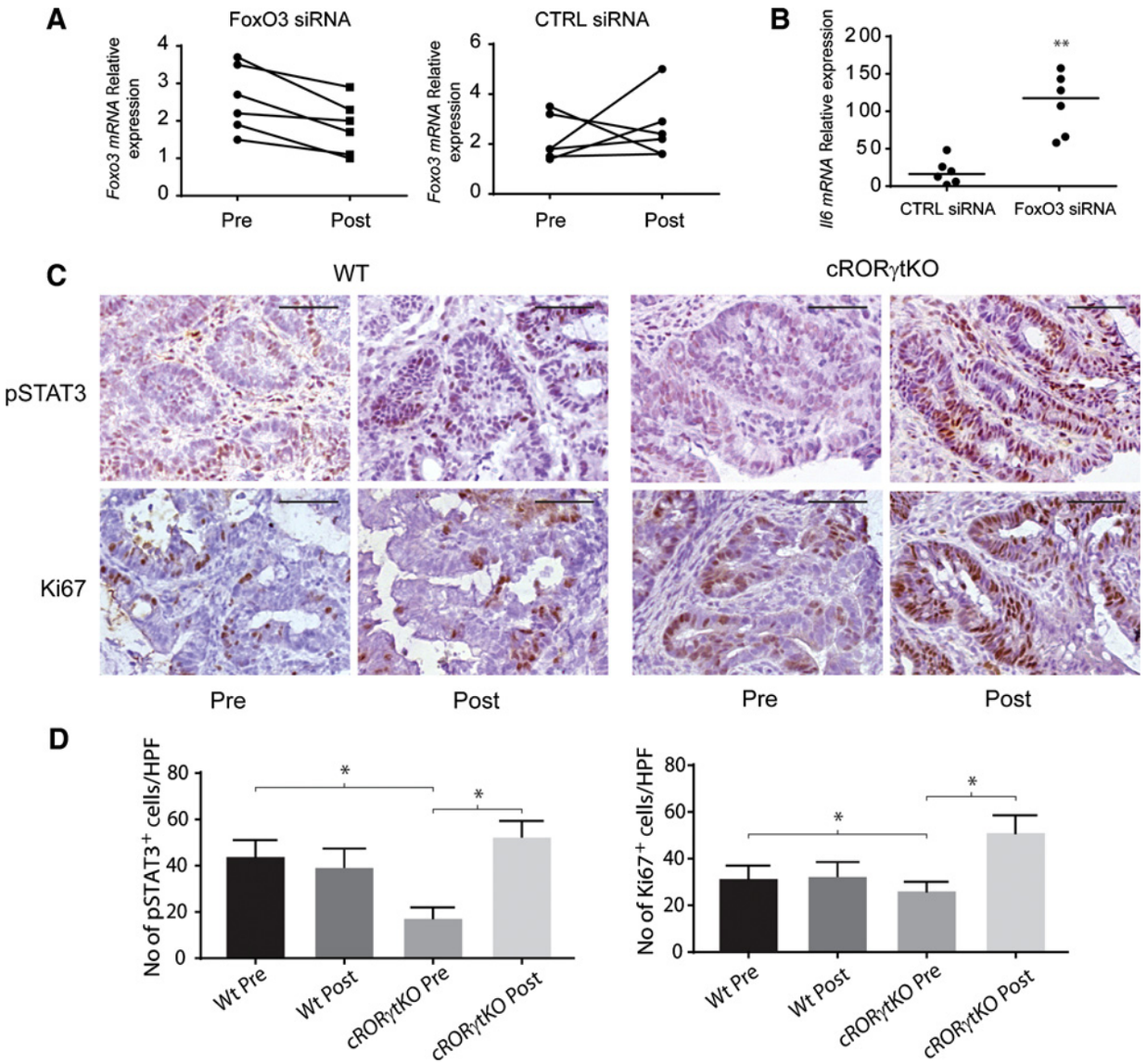

Figure 6.

In vivo suppression of intratumoral FoxO3 expression in cRORγtKO mice restores IL6 expression, STAT3 activation, and increases dysplastic cell proliferation. **A,** Expression of *Foxo3* mRNA expression in tumor biopsies of cRORγtKO mice ($n = 6$) before and 48 hours after injection of FoxO3 or control siRNA. **B,** *Il6* mRNA expression in tumors 48 hours after injection. **C,** Representative pSTAT3 and Ki67 immunohistochemical staining of tumor biopsies from WT ($n = 3$) and cRORγtKO ($n = 3$) mice collected before and 48 hours after injection of FoxO3 siRNA. Scale bars, 100 μm. **D,** Quantification of pSTAT3 and Ki67-positive cells from six HPF/section of tumor biopsies from three mice/group. Student *t* test was used; **, $P < 0.01$; *, $P < 0.05$.

tumors with FoxO3 or control siRNA at two different concentrations. *Foxo3* expression was evaluated by real-time PCR of RNA isolated from biopsies collected from the injected tumors at 24 and 48 hours after injection (Supplementary Fig. S5A). Because 10,000 nmol/L induced suppression as early as 24 hours, which was still observed at 48 hours after injection, this dose was used in the following experiments to assess the *in vivo* biologic effect of FoxO3 suppression (Supplementary Fig. S5B and S5C). Injection of cRORγtKO tumors with FoxO3, but not control, siRNA induced a significant reduction of *foxo3* expression compared with that expressed before injection (Fig. 6A). At the same time, tumors injected with FoxO3 siRNA showed a significant increase of IL6 mRNA as compared with controls (Fig. 6B). Finally, phosphorylated (p) STAT3 and the proliferation marker Ki67 were upregulated in tumors from cRORγtKO, but not WT, mice after injection with FoxO3 siRNA (Fig. 6C and D). Neither pSTAT3 nor Ki67 were upregulated after injection of control siRNA. These data confirmed *in vivo* the role of FoxO3 as a negative controller of IL6 expression, STAT3 activation, and proliferation of colonic tumors induced by inflammation.

Published OnlineFirst July 10, 2018; DOI: 10.1158/2326-6066.CIR-17-0698

Discussion

The accumulation of Tregs in cancer tissue has been associated with opposing prognostic outcomes. This might be explained by the presence of different Treg subsets. In inflammatory conditions, Tregs have been shown to acquire the expression of Th-related transcription factors in addition to FoxP3. During Th1-mediated inflammation, Tregs upregulate the Th1-specific transcription factor T-bet, leading to the expression of CXCR3 and the recruitment of FoxP3$^+$T-bet$^+$ Tregs at the site of inflammation (30, 31). Similarly, STAT3 expression by Tregs is required to control Th17-driven inflammation, whereas IRF4 in Tregs is pivotal to suppress a Th2-mediated immune response (32, 33). GATA3, involved in the differentiation of Th2 cells, contributes to the functional stability of Tregs (34, 35). These data suggest that in the tumor microenvironment, the activation of different transcriptional programs in Tregs might lead to different functional activities and, thus determining different prognostic outcomes.

Tregs coexpressing both FoxP3 and RORγt have been identified in both mice and humans. These cells are particularly enriched in the gut lamina propria and they have been shown to accumulate in IBD (16, 17). These cells are believed to represent an intermediate stage of differentiation between suppressive Tregs and pathogenic Th17 cells. The evidence that pathogenic Th17 cells derive from Tregs that have lost the expression of FoxP3 sustains the hypothesis that in inflammatory conditions, the suppressive phenotype of Tregs might be unstable (36, 37). Still, RORγt in Tregs can induce some of the functional features of Th17 cells (e.g., IL17A expression), leaving their suppressive capacity unaffected, thus indicating that in certain conditions, Tregs might functionally contribute to a Th17-related immune response (16).

Because Th17 cells are involved both in IBD and colorectal cancer development, this study was undertaken to investigate the contribution of FoxP3$^+$RORγt$^+$ Tregs to the initiation and progression of CAC. The reported data showed a significant accumulation of these cells in the dysplastic areas of colonic samples collected from patients affected by ulcerative colitis and complicated by CAC compared with the nondysplastic surrounding areas from the same samples. Similarly, in the AOM/DSS model of CAC, one third of the tumor-infiltrating RORγt$^+$CD4$^+$ T cells expressed FoxP3. However, only a small fraction of RORγt single-positive T cells were derived from Tregs that had lost FoxP3 expression, thus indicating that RORγt-expressing Tregs accumulated in the tumor do not represent an intermediate stage toward a Th17 phenotype and that these cells represent a stable subset of Tregs infiltrating the tumor tissue. These results are in agreement with the demonstration that FoxP3 is stably expressed in Tregs, and its downregulation occurs only in nonfully committed cells (38). Nevertheless, the expression of RORγt in tumor-infiltrating Tregs was not sufficient to induce a Th17-like phenotype, indicated by the low IL17A expression observed in these cells, further indicating that FoxP3$^+$RORγt$^+$ cells in the tumors are functionally distinct from the Th17 cells.

It has been reported that FoxP3$^+$RORγt$^+$ T cells have high secretion of anti-inflammatory IL10 and have a suppressive phenotype (11). FoxP3$^+$RORγt$^+$ T cells also show higher suppressive capacity compared with FoxP3$^+$RORγt$^-$ Tregs *in vivo* (16). In contrast, FoxP3$^+$RORγt$^+$ Tregs that are increased in the lamina propria of IBD patients have reduced suppressive capacity and enhanced expression of proinflammatory cytokines (17, 39). In our system, the specific deletion of RORγt in Tregs did not affect the grade of inflammation observed in the peritumoral areas, but it resulted in a reduction of tumor incidence and size. Therefore, RORγt-expressing Tregs promoted CAC development independently of their capacity to suppress colonic inflammation. Peritumoral inflammation in both WT and cRORγtKO mice was mild at the end of the experiment, when tumor incidence and growth was evaluated, and differences in the grade of inflammation at earlier time points could not be excluded.

The activation of the transcription factor STAT3 is critical for the proliferation of dysplastic cells, and the signals of many cytokine and growth factors converge on STAT3, thus contributing to colorectal cancer progression (40). IL6-mediated activation of STAT3 has been shown to be pivotal in CAC development. Inhibition of IL6 *trans*-signaling suppresses tumor growth in the AOM/DSS model of CAC (24, 41), and the proliferative and prosurvival effects of IL6 on tumor cells are mainly mediated by the activation of the transcription factor STAT3. STAT3 gain-of-function mice show increased CAC growth and multiplicity (25). In our model, proliferating Ki67$^+$ dysplastic cells were significantly lower in the cRORγtKO mice compared with WT, and this was associated with a reduced activation of STAT3 in the tumor cells. Among STAT3-activating cytokines, only IL6 was reduced in cRORγtKO mice. These data demonstrated that RORγt expression in Tregs was required to sustain the activation of the oncogenic IL6/STAT3 axis in dysplastic cells.

Flow cytometry analysis of TILs identified activated CD11c$^+$CD86$^+$ DCs as the major source of IL6, and the frequency of IL6-expressing CD11c$^+$CD86$^+$ cells in the dysplastic areas of cRORγtKO mice was reduced compared with WT mice. Although no difference in IL6 expression was observed among CD3$^+$ T cells, RORγt expression by tumor-infiltrating Tregs sustained IL6 expression indirectly by acting on DCs. In addition to the control of T-cell activation and differentiation, one of the key mechanisms by which Tregs mediate immune suppression is the control of DC function (28). Dejean and colleagues have shown a critical DC-intrinsic role of the transcription factor FoxO3 in the modulation of IL6 production (29). FoxO3 belongs to the forkhead family of transcription factors (i.e., FoxO1, FoxO4, and FoxO6), which are characterized by a distinct forkhead domain and act downstream of the phosphoinositol-3-kinase (PI3K)–AKT signaling cascade (42). Among the FoxO family members, FoxO3 contributes to the regulation of the immune system (43). Evidence obtained in FoxO3-deficient mice has shown that FoxO3 controls cytokine production, opposes NF-κB activation, suppresses T-cell activation and proliferation, and reduces the proliferation of lymphatic cells, resulting in a lower degree of inflammation (44). We demonstrated by *in vitro* and *in vivo* experiments that RORγt expression in Tregs is required to keep FoxO3 suppressed in tumor-infiltrating DCs, thus leaving IL6 expression in these cells unchecked. *In vitro*, cRORγtKO, but not WT, Tregs isolated from tumors suppressed IL6 expression in DCs activated by LPS, and this effect was reverted by FoxO3 silencing. Accordingly, *in vivo* silencing of FoxO3 in the tumors of cRORγtKO mice increased IL6 expression and led to increased STAT3 activation and expression of Ki67 in the tumors, further supporting that the protumorigenic effect of Treg-specific RORγt expression is mediated by the uncontrolled expression of IL6. These findings further strengthen the role of FoxO3 as a tumor suppressor in colorectal cancer. FoxO3 has been shown to induce autophagy, cell-cycle arrest, and apoptosis in colorectal cancer cell lines (45), and its activation has been linked to cisplatin responsiveness (46). Hence, our data extend the role of FoxO3 as a tumor suppressor to nondysplastic

Published OnlineFirst July 10, 2018; DOI: 10.1158/2326-6066.CIR-17-0698

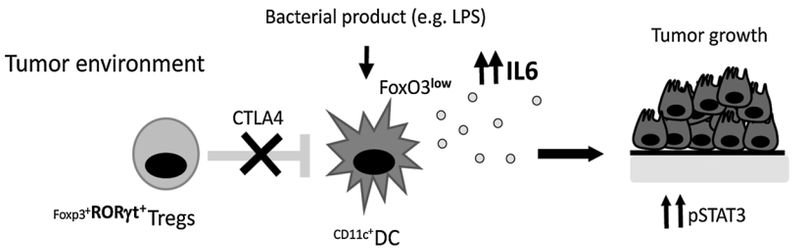

Figure 7.
Schematic interpretation of the data showing the role of RORγt expression in the tumor-infiltrating Tregs. Tumor-infiltrating FoxP3$^+$RORγt$^+$ Tregs suppress FoxO3 in DCs, leaving IL6 expression unchecked. At the same time, high IL6 promotes STAT3 activation and proliferation of dysplastic cells.

cells involving the control of IL6 expression in tumor-infiltrating DCs. Because in our model some FoxO3 expression was observed in the dysplastic cells, we cannot exclude that the increased expression of Ki67 after FoxO3 silencing could, at least in part, depend on a cell-intrinsic effect. However, FoxO3 suppression induced STAT3 activation, thus indicating that the activation of the IL6–STAT3 axis in these cells can substantially contribute to the increased proliferation observed.

FoxO3 has been shown to act downstream to CTLA-4–induced signals to constrain IL6 production in DCs (29). CTLA-4 is expressed on the cell membrane of regulatory T cells and is essential for suppression (47). CTLA-4 can also modify the function of DCs by triggering reverse signaling through CD80 and CD86 receptors, resulting in the production of suppressive mediators and/or the suppression of proinflammatory factors (48). Consistent with this, Tregs from the tumors of cRORγtKO mice showed increased expression of CTLA-4 compared with WT mice. *In vitro* neutralization of CTLA-4 completely reverted the suppression of IL6 operated by tumoral cRORγtKO Tregs. Although FoxP3$^+$RORγt$^+$ Tregs are characterized by higher expression of suppression-related markers, including CTLA-4 (16), in cRORγtKO mice we observed the upregulation of CTLA-4 in the whole FoxP3$^+$ cell population, thus suggesting that in the absence of RORγt, Tregs might upregulate CTLA-4 to compensate for the loss of suppressive RORγt$^+$ Tregs. We currently do not know the mechanism of how the absence of RORγt$^+$ Tregs can influence the expression of suppressive molecules on the surface of the remaining Tregs and warrants further investigation.

Overall, our data demonstrated that Tregs coexpressing the transcription factors FoxP3 and RORγt reduced Foxo3 expression in tumor-infiltrating DCs, leaving IL6 expression unchecked. In turn, high IL6 expression in the tumor microenvironment, as previously demonstrated (25, 41), drove STAT3 activation and proliferation of dysplastic cells and promoted CAC growth (Fig. 7). In agreement with our findings, previously published data demonstrate that the expression of RORγt by Tregs in APC$^{min/+}$ mice, which spontaneously develop multiple colonic tumors in the absence of colitis, is required to induce the expression of proinflammatory cytokines in the tumor microenvironment (18).

Initially, believed as a static subpopulation of T cells characterized by suppressive capacity, Tregs are now emerging as functionally plastic cells able to exert different immunosuppressive effects in a context-dependent manner. The expression of different transcription factors in Tregs has been associated with the ability to suppress specific immune responses and to govern the dissociation between the negative control on T-cell proliferation and proinflammatory properties. Our data extend this concept to CAC, where the expression of the transcription factor RORγt specifically allows IL6 expression by tumor-infiltrating DCs, thus contributing to tumor growth.

Disclosure of Potential Conflicts of Interest

No potential conflicts of interest were disclosed.

Authors' Contributions

Conception and design: A. Rizzo, M.C. Fantini
Development of methodology: A. Rizzo, E. Franzè, M. Rugge
Acquisition of data (provided animals, acquired and managed patients, provided facilities, etc.): A. Rizzo, M. Di Giovangiulio, R. Carsetti, E. Giorda, M. Rugge, C. Mescoli
Analysis and interpretation of data (e.g., statistical analysis, biostatistics, computational analysis): A. Rizzo, M. Di Giovangiulio, M.C. Fantini
Writing, review, and/or revision of the manuscript: A. Rizzo, M. Di Giovangiulio, M.C. Fantini
Administrative, technical, or material support (i.e., reporting or organizing data, constructing databases): A. Rizzo, H.-J. Fehling
Study supervision: M.C. Fantini
Other (collected, acquired, and analyzed data and to wrote the manuscript): M. Di Giovangiulio
Other (real-time PCR): C. Stolfi
Other (protein analysis): E. Franzè
Other (provision of ROSA-tdRFP mouse mutants): H.-J. Fehling
Other (IHC): A. Colantoni, A. Ortenzi
Other (revision of the manuscript): G. Monteleone

Acknowledgments

This study was supported by Associazione Italiana per la Ricerca sul Cancro (AIRC) IG13304, Futuro in Ricerca, MIUR, RBFR12VP3Q, and Giovani ricercatori, Ministero della Salute GR-2011-02348069. We acknowledge Prof. Alexander Rudensky (HHMI, MD) for kindly providing the FoxP3-eGFPCre knockin mice.

The costs of publication of this article were defrayed in part by the payment of page charges. This article must therefore be hereby marked *advertisement* in accordance with 18 U.S.C. Section 1734 solely to indicate this fact.

Received December 2, 2017; revised April 17, 2018; accepted July 5, 2018; published first July 10, 2018.

References

1. Eaden JA, Abrams KR, Mayberry JF. The risk of colorectal cancer in ulcerative colitis: a meta-analysis. Gut 2001;48:526–35.
2. Rutter MD, Saunders BP, Wilkinson KH, Schofield GL, Rumbles SW, Forbes A. Severity of colonic inflammation is a risk factor for dysplasia in ulcerative colitis. Gastroenterology 2003;124:A207–A.
3. Boehm F, Martin M, Kesselring R, Schiechl G, Geissler EK, Schlitt HJ, et al. Deletion of Foxp3+ regulatory T cells in genetically targeted mice supports development of intestinal inflammation. BMC Gastroenterol 2012;12:97.
4. Hori S, Nomura T, Sakaguchi S. Control of regulatory T cell development by the transcription factor Foxp3. Science 2003;299:1057–61.

5. Tosolini M, Kirilovsky A, Mlecnik B, Fredriksen T, Mauger S, Bindea G, et al. Clinical impact of different classes of infiltrating T cytotoxic and helper cells (Th1, th2, treg, th17) in patients with colorectal cancer. Cancer Res 2011; 71:1263–71.
6. Correale P, Rotundo MS, Del Vecchio MT, Remondo C, Migali C, Ginanneschi C, et al. Regulatory (FoxP3+) T-cell tumor infiltration is a favorable prognostic factor in advanced colon cancer patients undergoing chemo or chemoimmunotherapy. J Immunother 2010;33:435–41.
7. Salama P, Phillips M, Grieu F, Morris M, Zeps N, Joseph D, et al. Tumor-infiltrating FOXP3+ T regulatory cells show strong prognostic significance in colorectal cancer. J Clin Oncol 2009;27:186–92.
8. Sinicrope FA, Rego RL, Ansell SM, Knutson KL, Foster NR, Sargent DJ. Intraepithelial effector (CD3+)/regulatory (FoxP3+) T-cell ratio predicts a clinical outcome of human colon carcinoma. Gastroenterology 2009;137: 1270–9.
9. Erdman SE, Rao VP, Poutahidis T, Ihrig MM, Ge Z, Feng Y, et al. CD4(+) CD25(+) regulatory lymphocytes require interleukin 10 to interrupt colon carcinogenesis in mice. Cancer Res 2003;63:6042–50.
10. Chang LY, Lin YC, Mahalingam J, Huang CT, Chen TW, Kang CW, et al. Tumor-derived chemokine CCL5 enhances TGF-beta-mediated killing of CD8(+) T cells in colon cancer by T-regulatory cells. Cancer Res 2012; 72:1092–102.
11. Lochner M, Peduto L, Cherrier M, Sawa S, Langa F, Varona R, et al. In vivo equilibrium of proinflammatory IL-17+ and regulatory IL-10+ Foxp3+ RORgamma t+ T cells. J Exp Med 2008;205:1381–93.
12. Ivanov II, McKenzie BS, Zhou L, Tadokoro CE, Lepelley A, Lafaille JJ, et al. The orphan nuclear receptor RORgammat directs the differentiation program of proinflammatory IL-17+ T helper cells. Cell 2006;126:1121–33.
13. Bailey-Bucktrout SL, Martinez-Llordella M, Zhou X, Anthony B, Rosenthal W, Luche H, et al. Self-antigen-driven activation induces instability of regulatory T cells during an inflammatory autoimmune response. Immunity 2013;39:949–62.
14. Komatsu N, Okamoto K, Sawa S, Nakashima T, Oh-hora M, Kodama T, et al. Pathogenic conversion of Foxp3+ T cells into TH17 cells in autoimmune arthritis. Nat Med 2014;20:62–8.
15. Zhou X, Bailey-Bucktrout SL, Jeker LT, Penaranda C, Martinez-Llordella M, Ashby M, et al. Instability of the transcription factor Foxp3 leads to the generation of pathogenic memory T cells in vivo. Nat Immunol 2009;10: 1000–7.
16. Yang BH, Hagemann S, Mamareli P, Lauer U, Hoffmann U, Beckstette M, et al. Foxp3(+) T cells expressing RORgammat represent a stable regulatory T-cell effector lineage with enhanced suppressive capacity during intestinal inflammation. Mucosal Immunol 2016;9:444–57.
17. Ueno A, Jijon H, Chan R, Ford K, Hirota C, Kaplan GG, et al. Increased prevalence of circulating novel IL-17 secreting Foxp3 expressing CD4+ T cells and defective suppressive function of circulating Foxp3+ regulatory cells support plasticity between Th17 and regulatory T cells in inflammatory bowel disease patients. Inflamm Bowel Dis 2013;19:2522–34.
18. Blatner NR, Mulcahy MF, Dennis KL, Scholtens D, Bentrem DJ, Phillips JD, et al. Expression of RORgammat marks a pathogenic regulatory T cell subset in human colon cancer. Sci Transl Med 2012;4:164ra59.
19. Becker C, Fantini MC, Neurath MF. High resolution colonoscopy in live mice. Nat Protoc 2006;1:2900–4.
20. Ito R, Shin-Ya M, Kishida T, Urano A, Takada R, Sakagami J, et al. Interferon-gamma is causatively involved in experimental inflammatory bowel disease in mice. Clin Exp Immunol 2006;146:330–8.
21. Grivennikov S, Karin E, Terzic J, Mucida D, Yu GY, Vallabhapurapu S, et al. IL-6 and Stat3 are required for survival of intestinal epithelial cells and development of colitis-associated cancer. Cancer Cell 2009;15:103–13.
22. Stolfi C, Rizzo A, Franze E, Rotondi A, Fantini MC, Sarra M, et al. Involvement of interleukin-21 in the regulation of colitis-associated colon cancer. J Exp Med 2011;208:2279–90.
23. Yu H, Kortylewski M, Pardoll D. Crosstalk between cancer and immune cells: role of STAT3 in the tumour microenvironment. Nat Rev Immunol 2007;7:41–51.
24. Becker C, Fantini MC, Wirtz S, Nikolaev A, Lehr HA, Galle PR, et al. IL-6 signaling promotes tumor growth in colorectal cancer. Cell Cycle 2005; 4:217–20.
25. Bollrath J, Phesse TJ, von Burstin VA, Putoczki T, Bennecke M, Bateman T, et al. gp130-mediated Stat3 activation in enterocytes regulates cell survival and cell-cycle progression during colitis-associated tumorigenesis. Cancer Cell 2009;15:91–102.
26. De Simone V, Franze E, Ronchetti G, Colantoni A, Fantini MC, Di Fusco D, et al. Th17-type cytokines, IL-6 and TNF-alpha synergistically activate STAT3 and NF-kB to promote colorectal cancer cell growth. Oncogene 2015;34:3493–503.
27. Khare V, Paul G, Movadat O, Frick A, Jambrich M, Krnjic A, et al. IL10R2 overexpression promotes IL22/STAT3 signaling in colorectal carcinogenesis. Cancer Immunol Res 2015;3:1227–35.
28. Onishi Y, Fehervari Z, Yamaguchi T, Sakaguchi S. Foxp3+ natural regulatory T cells preferentially form aggregates on dendritic cells in vitro and actively inhibit their maturation. Proc Natl Acad Sci U S A 2008;105:10113–8.
29. Dejean AS, Beisner DR, Ch'en IL, Kerdiles YM, Babour A, Arden KC, et al. Transcription factor Foxo3 controls the magnitude of T cell immune responses by modulating the function of dendritic cells. Nat Immunol 2009;10:504–13.
30. Koch MA, Thomas KR, Perdue NR, Smigiel KS, Srivastava S, Campbell DJ. T-bet(+) Treg cells undergo abortive Th1 cell differentiation due to impaired expression of IL-12 receptor beta2. Immunity 2012;37:501–10.
31. Koch MA, Tucker-Heard G, Perdue NR, Killebrew JR, Urdahl KB, Campbell DJ. The transcription factor T-bet controls regulatory T cell homeostasis and function during type 1 inflammation. Nat Immunol 2009;10:595–602.
32. Chaudhry A, Rudra D, Treuting P, Samstein RM, Liang Y, Kas A, et al. CD4+ regulatory T cells control TH17 responses in a Stat3-dependent manner. Science 2009;326:986–91.
33. Zheng Y, Chaudhry A, Kas A, deRoos P, Kim JM, Chu TT, et al. Regulatory T-cell suppressor program co-opts transcription factor IRF4 to control T(H)2 responses. Nature 2009;458:351–6.
34. Wang Y, Su MA, Wan YY. An essential role of the transcription factor GATA-3 for the function of regulatory T cells. Immunity 2011;35:337–48.
35. Wohlfert EA, Grainger JR, Bouladoux N, Konkel JE, Oldenhove G, Ribeiro CH, et al. GATA3 controls Foxp3(+) regulatory T cell fate during inflammation in mice. J Clin Invest 2011;121:4503–15.
36. Zhou L, Chong MM, Littman DR. Plasticity of CD4+ T cell lineage differentiation. Immunity 2009;30:646–55.
37. Zhou X, Bailey-Bucktrout S, Jeker LT, Bluestone JA. Plasticity of CD4(+) FoxP3(+) T cells. Curr Opin Immunol 2009;21:281–5.
38. Miyao T, Floess S, Setoguchi R, Luche H, Fehling HJ, Waldmann H, et al. Plasticity of Foxp3(+) T cells reflects promiscuous Foxp3 expression in conventional T cells but not reprogramming of regulatory T cells. Immunity 2012;36:262–75.
39. Kryczek I, Wu K, Zhao E, Wei S, Vatan L, Szeliga W, et al. IL-17+ regulatory T cells in the microenvironments of chronic inflammation and cancer. J Immunol 2011;186:4388–95.
40. Grivennikov SI, Greten FR, Karin M. Immunity, inflammation, and cancer. Cell 2010;140:883–99.
41. Becker C, Fantini MC, Schramm C, Lehr HA, Wirtz S, Nikolaev A, et al. TGF-beta suppresses tumor progression in colon cancer by inhibition of IL-6 trans-signaling. Immunity 2004;21:491–501.
42. Myatt SS, Lam EW. The emerging roles of forkhead box (Fox) proteins in cancer. Nat Rev Cancer 2007;7:847–59.
43. Becker T, Loch G, Beyer M, Zinke I, Aschenbrenner AC, Carrera P, et al. FOXO-dependent regulation of innate immune homeostasis. Nature 2010; 463:369–73.
44. Lin L, Hron JD, Peng SL. Regulation of NF-kappaB, Th activation, and autoinflammation by the forkhead transcription factor Foxo3a. Immunity 2004;21:203–13.
45. Chiacchiera F, Matrone A, Ferrari E, Ingravallo G, Lo Sasso G, Murzilli S, et al. p38alpha blockade inhibits colorectal cancer growth in vivo by inducing a switch from HIF1alpha- to FoxO-dependent transcription. Cell Death Differ 2009;16:1203–14.
46. Fernandez de Mattos S, Villalonga P, Clardy J, Lam EW. FOXO3a mediates the cytotoxic effects of cisplatin in colon cancer cells. Mol Cancer Ther 2008;7:3237–46.
47. Wing K, Onishi Y, Prieto-Martin P, Yamaguchi T, Miyara M, Fehervari Z, et al. CTLA-4 control over Foxp3+ regulatory T cell function. Science 2008; 322:271–5.
48. Orabona C, Grohmann U, Belladonna ML, Fallarino F, Vacca C, Bianchi R, et al. CD28 induces immunostimulatory signals in dendritic cells via CD80 and CD86. Nat Immunol 2004;5:1134–42.

AACR American Association for Cancer Research

Cancer Immunology Research

RORγt-Expressing Tregs Drive the Growth of Colitis-Associated Colorectal Cancer by Controlling IL6 in Dendritic Cells

Angelamaria Rizzo, Martina Di Giovangiulio, Carmine Stolfi, et al.

Cancer Immunol Res 2018;6:1082-1092. Published OnlineFirst July 10, 2018.